Supplementary Material: NOX4-dependent neuronal autotoxicity and blood-brain barrier breakdown explain the superior sensitivity of the brain to ischemic damage

Ana I Casas[a,1], Eva Geuss[b,1], Pamela WM Kleikers[a], Stine Mencl[c], Alexander M. Herrmann[d], Izaskun Buendia[e], Javier Egea[f], Sven G. Meuth[d], Manuela G Lopez[e], Christoph Kleinschnitz[b,c,2,*], Harald HHW Schmidt[a,2,*]

[a]Department of Pharmacology & Personalised Medicine, CARIM, Maastricht University, Universiteitssingel 50, 6229 ER Maastricht, The Netherlands; [b]Department of Neurology, University Hospital Würzburg, Josef-Schneider-Straße 2, 97080 Würzburg, Germany; [c]Department of Neurology, University Clinics Essen, Hufelandstraße 55 D-45147 Essen, Germany. [d]Department of Neurology, Westfälische Wilhelms-Universität Münster, Münster, Germany. [e]Department of Pharmacology, School of Medicine, Universidad Autónoma de Madrid, Arzobispo Morcillo s/n, 28029 Madrid, Spain; [f]Instituto de Investigación Sanitaria, Servicio de Farmacología Clínica, Hospital Universitario de la Princesa, 28006 Madrid, Spain; [1]Both first authors contributed equally to this work. [2]Both senior authors contributed equally to this work.

[*]To whom correspondence should be addressed: h.schmidt@maastrichtuniversity.nl and christoph.kleinschnitz@uk-essen.de

Key words: Stroke, NOX4, blood-brain barrier, neuronal autotoxicity

Supplementary Materials and Methods

Animals

All animal experiments were approved by local state authorities (Regierung von Unterfranken), comply with the ARRIVE guidelines and are carried out in accordance with the EU Directive 2010/63/EU for animal experiments as well as the German Animal Welfare Act (German Ministry of Agriculture, Health and Economic Cooperation), the Dutch law on animal experiments and were approved by the Ethics Committee of Faculty of Medicine, Universidad Autónoma de Madrid (Madrid, Spain). Animals were housed under controlled conditions (22°C, 55–65% humidity, 12h light-dark cycle), and were allowed free access to water and standard laboratory chow. Male and female mice aged 8-16 weeks and adult rats (>12 weeks) were used. The Nox4 KO animals were compared to their respective matched WT's.

NOX4 expression in different ischemia models

Muscle from the lower leg from wild type mice subjected to a permanent ligation of the femoral artery and heart apex after occlusion of the left descending coronary artery were collected together with tissue samples from matched non-ischemic mice. Brain tissue from stroked and non-stroked brain areas were collected and snap-frozen. Similarly, human brain microvascular endothelial cells were collected following the hypoxia period. After homogenization, total mRNA was prepared by using the TRI Reagent® (Sigma-Aldrich, The Netherlands) and was quantified spectrophotometrically. 0.08 µg of total mRNA was reverse transcribed to cDNA with the High Capacity Reverse Transcription Kit (Applied Biosystems, The Netherlands) according to the manufacturer's protocol. mRNA levels of *Nox4* were quantified by using the fluorescent Taqman® technology. *Cyplophilin* and *Gapdh* were used as reference genes for the *in vivo* and *in vitro* models respectively. We used TaqMan®

gene expression arrays (TaqMan® Universal PCR Master Mix, ThermoFisher Scientific, The Netherlands) specific for mouse: *Nox4* (Mm00479246_m1, ThermoFisher Scientific, The Netherlands), mouse *Cyclophilin* (Mm02342430_g1, ThermoFisher Scientific, The Netherlands), *Gapdh* (Mm99999915_g1, ThermoFisher Scientific, The Netherlands) and human: *Nox4* (Hs00418353_m1, ThermoFisher Scientific, The Netherlands), *Gapdh* (Hs02758991_g1, ThermoFisher Scientific, The Netherlands). Water controls were included to ensure specificity and the comparative ΔΔCt method was used for relative quantification of gene expression.

Cell specific Nox4 KO mice generation

Constitutive Nox4 KO mice and floxed Nox4 mice were generated as described (1). To generate endothelial-specific Nox4 KO (eNox4 KO) mice, female mice (homozygous for the floxed NOX4 gene) were bred with male mice (C57Bl6 strain background) that express the Cre recombinase gene under control of the endothelial-cell specific Tie2 promotor (2). As the Cre is located on the X chromosome, all males used for this breeding were hemizygous for the Cre gene ($Cre^{+/y}$). During breeding, only males that bear the Cre gene were selected for future breeding rounds, while females were not allowed to bear the Cre. For experiments Cre positive (eNox4 KO) males were used. Smooth muscle cell-specific and neuron specific Nox4 KO mice were generated in an analogous way using SMMHC-CreERT2 mice (2) and CamKII Cre (3) (EMMA ID number 01153) mice respectively. Deletion of NOX4 in SMC and neurons was induced using Tamoxifen as described (4). For tMCAO, male 8-10 weeks old Cre positive mice treated with tamoxifen (sNox4 KO and nNox4 KO) were used. For all three lines Cre negative NOX4FF mice were used as controls (WT), with the WT groups for the SMC and neuron specific lines also being injected with tamoxifen.

Verification of NOX4 deficiency in eKO, nKO and sKO mice

Histology and immunohistochemistry were performed according to standard procedures (5). The cell-specific Nox4 KO mice validation was performed on formalin fixed paraffin embedded tissue (brain or aorta) that was pre-treated with Proteinase K prior to antibody incubation. For specific staining, the following antibodies were used: pAb anti -CD31 (Biorad, MCA2388), NOX4 (kindly provided by A.M. Shah, King's College London British Heart Foundation Centre, London) and anti-NeuN (Millipore, MAB337). DNA was visualized with Hoechst and sections were coverslipped using Aqua Poly Mount. All sections were analyzed with a Nikon Eclipse 50 microscope equipped with the DS-U3 DS camera control unit and NIS- Elements software (Nikon, Tokyo, Japan).

NOX4 expression in bone marrow flushes

Bone marrow samples from endothelial NOX4 KO and their respective WT mice were collected. mRNA isolation and cDNA preparation were prepared as previously described. mRNA levels of *Nox4* were quantified by using the fluorescent Taqman® technology. *ß-actin* were used as reference gene. We used TaqMan® gene expression arrays (TaqMan® Universal PCR Master Mix, ThermoFisher Scientific, The Netherlands) specific for mouse: *Nox4* (Mm00479246_m1, ThermoFisher Scientific, The Netherlands), *Nox2* (Mm1287743_m1, ThermoFisher Scientific, The Netherlands) and *ß-actin* (Mm02619580_g1, ThermoFisher Scientific, The Netherlands). Water controls were included to ensure specificity.

Nox4 KO rat generation

Nox4 KO rats were generated at Sage Labs using the CompoZr Zinc Finger Nuclease technology. The E14-15 domain (2.3-2.4 Kb) of the *Nox4* gene was removed in a WKY background rat. Zinc-Finger Nucleases (ZFNs) were coupled with a FOK1

endonuclease and designed to recognize and cleave the specific NOX4 sequence producing sequence-specific double-strand breaks that are repaired by error-prone non-homologous end joining (NHEJ) or high-fidelity homologous recombination (HR). The Nox4 KO rat was generated by introducing variable genomic deletions that result in a frameshift within the open reading frame. The frameshifts often result in the introduction of a premature stop codon. When the premature stop codon occurs before the last exon, the transcript is likely degraded via nonsense mediated decay pathway and little or no protein is expressed. Resulting animals were screened for mutations and complete genomic sequencing was performed.

Nox4 KO rat genotyping

DNA isolation and PCR from rat tail cuts was performed using the Quanta Bioscoences AccuStart II Rat/Mouse genotyping kit (VWR cat no. 95135-500) according to the instructions from the manufacturer with the following primers: forward Int13 Cel1. 5'-TGTCTGCCAGAGCATTCACTA-3', reverse Int13 Cel1 5'-CAAATGGACTTCCAAATGGG-3' and reverse Int15 Cel1 5'-CTTCTGCAGTCTACCCTGGC-3'. A 2% Agarose gel was used, running for 45-50 minutes. Expected PCR products are 383bp for WT and 300bp for KO.

Verification of NOX4 deficiency in Nox4 KO rats

Brain, kidney and lung tissue were collected from WT and Nox4 KO rats. mRNA isolation and cDNA preparation were prepared as previously described. mRNA levels of *Nox1, Nox2* and *Nox4* in brain, kidney and lung were quantified by using the fluorescent Taqman® technology. We used TaqMan® gene expression arrays (TaqMan® Universal PCR Master Mix, ThermoFisher Scientific, The Netherlands) specific for rat *Nox1* (Rn00586652_m1, ThermoFisher Scientific, The Netherlands), *Nox2* (Rn00576710_m1, ThermoFisher Scientific, The Netherlands) and *Nox4*

(Rn01506793_m1, ThermoFisher Scientific, The Netherlands). Water controls were included to ensure specificity and the comparative ΔCt method was used for relative quantification of gene expression.

Stroke surgery (tMCAO model)

The model has previously been established as described in (1) for mice and (6) rat surgery. Animals were anesthetized with isoflurane (2-2.5% in oxygen). The animal was placed on a heating-pad, and rectal temperature was maintained at 37.0°C using a feedback-controlled infrared lamp. Focal cerebral ischemia was induced using an intraluminal filament technique. Using a surgical microscope (Wild M5A, Wild Heerbrugg, Gais, CH), a midline neck incision was made and the right common and external carotid arteries were isolated and permanently ligated. A microvascular clip was temporarily placed on the internal carotid artery. A silicon rubber-coated 6.0 nylon monofilament (602312PK10, Doccol Corporation, Sharon, MA, USA) for mice and 4.0 nylon monofilament (40SP, Doccol Corporation, Sharon, MA, USA) for rats was inserted through a small incision into the common carotid artery and advanced into the internal carotid artery until a resistance is felt. The tip of the monofilament should be located intracranially at the origin of the right middle cerebral artery and thereby interrupting blood flow. The filament was held in place by a tourniquet suture that has been prepared before to prevent dislocation during the ischemia period and the wound was closed. Reperfusion was initiated 1 hour after occlusion by monofilament removal in mice and 1.5h for rat experiments. After the surgery, wounds were carefully sutured and animals were allowed to recover from surgery in a temperature-controlled cupboard. Animals were excluded from the stroke analysis, if animals died before the predefined experimental end point, if an intracerebral hemorrhage occurred, if the

animal lost more than 20% of body weight or if the animal scored 0 on the Bederson score (**SI Appendix, Table S3**).

Treatment with NOX inhibitor: GKT136901

GKT136901 was dissolved in a mixture of DMSO/water in a ratio of 1/99. GKT136901 (10 mg/kg) or vehicle (DMSO/water in a ratio of 1/99) were injected i.p. 1 h after removal of the filament, i.e. 2 h after induction of tMCAO.

Brain infarct volume measurements

The ischemic lesion was measured 24 hours after MCAO using TTC staining (6). The brain was cut in three (mice) or five (rats) 2mm thick coronal sections using a mouse/rat brain slice matrix (Harvard Apparatus, Holliston, MA, USA). The slices were soaked for 10 min in a freshly-prepared solution of 2% 2,3,5- triphenyltetrazolium hydrochloride (TTC, Sigma-Aldrich Chemie GmbH, Munich, Germany. Total indirect (i.e corrected for brain edema) infarct volume was calculated by volumetry (ImageJ 1.49 software, National Institutes of Health) according to the formula: $V_{indirect}$ (mm^3) = $V_{infarct}$ x (1-(V_{ih}-V_{ch}) / V_{ch}, where the term V_{ih}-V_{ch} represents the volume difference between the ipsilateral and contralateral hemisphere and (V_i-V_c) / V_c expresses this difference as % of the control hemisphere. Brain edema volume can be calculated by subtracting corrected from uncorrected infarct volumes (7).

Neurological behaviour

The mice were assessed for neurological behaviour just before sacrifice to determine the final functional status. Neurological deficits were measured in a blinded manner on a 0 to 5 scale using the Bederson Score (8) with the following definitions for mice and rats:

Mice: Score 0, no apparent neurological deficits; 1, body torsion and forelimb flexion; 2, right side weakness and thus decreased resistance to lateral push; 3, unidirectional circling behaviour; 4, longitudinal spinning; 5, no movement.

Rat: Score 0, no deficits; 1, flexion of the left forelimb; 2, flexion of the left forelimb and right side weakness; 3, occasional unidirectional circling behaviour; 4, occasional circling and longitudinal spinning; 5 no movement.

Motor function

Prior to sacrifice, the mice and rats were also scored for neurological motor deficits according to the Grip Test (9). Each mouse was given a discrete value from 0 to 5. This score is used to evaluate motor function and coordination. The apparatus is a metal rod (0.22 cm diameter, 50cm length) between two vertical supports at a height of 40 cm over a flat surface. The animal is placed mid-way on this rod and is rated according to the following system: Score 0, falls off; 1, hangs on to string by one or both fore paws; 2, as for 1, and attempts to climb on to string; 3, hangs on to string by one or both fore paws plus one or both hind paws; 4, hangs on to string by fore and hind paws plus tail wrapped around string; 5, escape (towards the supports).

Protein Extraction and Western Blot Analysis

Western blot analysis was performed according to standard procedures (10). The following primary antibodies were used: polyclonal antibody (pAb) anti-occludin (ab31721, Abcam), and mAb anti–b-actin (A5441, Sigma-Aldrich).

Blood-brain barrier function

To determine the permeability of the cerebral vasculature and brain edema, 2% Evans blue tracer (Sigma Aldrich, Germany) diluted in 0.9% NaCl was injected intravenously at reperfusion. Measurement of Evans Blue extravasation was performed as described in (1).

Oxidative stress: DHE staining

The presence of ROS was determined using dihydroethidium (Sigma, stock solution 2mM) staining in coronal brain sections taken from identical regions (-0.5mm from bregma) of the different animal groups. Briefly, frozen sections were incubated in 2µM DHE for 30 minutes at 37°C, washed three times with PBS and incubated with Hoechst (Hoechst 33342, Sigma-Aldrich) 2ng/ml for 10 min. All sections were analyzed and acquired with a Nikon Eclipse 50i microscope equipped with the DS-U3 DS camera control unit. The relative pixel intensity was measured in identical regions with NIS-Elements software (Nikon, Tokyo, Japan). Digital images were processed using Adobe Photoshop (Adobe Systems, San Jose, CA).

Cell death measurement

Apoptotic neurons were visualized by TUNEL analysis on cryopreserved brain sections as described in (11). The TUNEL *in situ* death detection kit TMR red (Roche, Switzerland) was used according to the manufacturer's instructions. Afterwards, slices were washed and subsequently covered with AquaTec (Merck, Darmstadt, Germany). All sections were analyzed with a Nikon Eclipse 50i microscope equipped with the DS-U3 DS camera control unit and NIS- Elements software (Nikon, Tokyo, Japan). Digital images were processed using Adobe Photoshop (Adobe Systems, San Jose, CA). Necrotic Neurons were visualized by Fluoro-Jade C (#AG325, Millipore) staining on paraffin embedded brain sections. The Fluoro-Jade C staining was performed as suggested by the manufacturer. Afterwards, slices were washed and stained with DAPI (1:1000 in PBS, #D9542, Sigma-Aldrich) and subsequently covered with CYTOSEAL XYL (8312-4 Thermo Scientific. All pictures where made with a DMi8 microscope (Leica Microsystems, Wetzlar) equipped with a Hamamatsu Orca Flash 4.0 V2 Camera (Hamamatsu, Herrsching) and the LASX software (Leica

Microsystems). For cell counting and picture processing ImageJ (NIH, version 1.51p) was used.

Murine model of hindlimb ischemia

The right femoral artery was permanently ligated**.** The mouse was placed on a heating pad (UNO temperature control unit, UNO Roestvaststaal BV) and body temperature was monitored using a rectal probe and maintained at 37°C using a feedback-controlled infrared lamp. A suture (5-0 silk) was placed around the femoral artery in between the branching of the a. epigastrica and the a. poplitea. These last two arteries were also ligated to prevent collateral flow and backflow respectively. The wound was then closed with a 4-0 polysorb suture. Animals were sacrificed 4 weeks after femoral artery ligation.

In the study, 23 WT and 17 KO animals were used. Two of the 25 WT animals died due to bleeding complications during the surgery. A Doppler measurement after the surgery was performed to exclude animals with no cessation of blood flow (**SI Appendix, Table S3**). This post-doppler measurement confirmed correct ligation of the artery and thus cessation of the blood flow in all of the animals.

Doppler measurements

Doppler measurements were done before and directly after surgery, at day 3, day 14 and day 28 after surgery. Mice were anesthetized and placed on the heating plate of the Moor Laser-Doppler (Moor LDI2™, Moor Instruments LtD Millwey Axminster Devon UK). The mouse was allowed to heat up for 10 minutes before starting the scan. Three consecutive scans were made for each mouse. An area of interest was drawn around the paws and the mean color pixel value was calculated per paw and expressed as ratio of ligated over non-ligated leg.

Capillary density

Muscle samples were dissected and formalin-fixed. Paraffin embedded sections (4µm) of the musculus adductor and musculus gastrocnemius were used for CD31 staining. Antigen retrieval was achieved by heat induced epitope retrieval using 0.01 M Citrate buffer (pH 6.0). Slides were incubated at 4°C overnight with the primary antibody, monoclonal rat anti-mouse antibody to CD31 (PECAM-1) (Histonova-Dianova, Cat. no DIA310) diluted 1:50. As secondary antibody, biotin labelled rabbit anti-rat antibody (dakocytomotion Denmark no. E0468) was used diluted 1:200 (incubation for 30 minutes). Pictures were taken using a Leica camera connected to a Zeiss microscope. Pictures were analysed using the Leica Qwin pro v3.5.1 software. For each animal, three random pictures were taken per muscle sample and the amount of capillaries is expressed as number per square mm.

Myocardial infarction and ischemia-reperfusion of the heart models

Mice were anaesthetized with isoflurane in air (Abbott forene Isoflurane, 4-5% for induction, 2-3% for maintenance) and intubated per orally with a stainless-steel tube connected to a respirator (rodent ventilator Microvent type 845, Hugo Sachs Electronic, Germany), set at a stroke volume of 250µL and a rate of 210 strokes/min. Body temperature was monitored using a rectal probe and maintained at 37.0°C using a feedback-controlled infrared lamp and a heating plate. During surgery, an ECG was recorded with IDEEQ software (IDEE, Maastricht University). Using a left thoracotomy, the left descending coronary artery (LAD) was ligated with a 6-0 polyprolene suture permanently for myocardial infarction (MI). For the transient ischemia of 45 minutes, a small poly-ethylene tube was inserted under the ligature, compressing the coronary artery, which was then removed after the ischemic period. During the ischemic period, mice were kept under anesthesia. The chest was closed with 5-0 silk sutures (Ethicon).

The animals were weaned from the respirator and the endotracheal tube was removed, once the mice breathed spontaneously. After surgery, mice were allowed to recover in a thermoneutral temperature (28 °C). After 24 hours (short term transient ischemia), an ultrasound was performed followed by terminal hemodynamic characterisation (see below), then the heart was excised and used for infarct size measurements (see below TTC stain). At the end of the long-term experiment (28 days), hearts were quickly excised and the atria were removed. The ventricles were cut transversally at 3mm from the apex. The apical part was shock frozen for mRNA extraction. The basal part was fixed in formalin and processed for paraffin embedding.

Animals included

Short term study: In total, 46 KO and 48 WT animals were included in the complete study. For infarct size measurements, 19 WT and 18 KO animals were used. For one KO animal no reperfusion was seen, one WT animal did not have a visible ischemia and 3 WT animals died during surgery or before the endpoint of 24h. The remaining 17 WT and 16 KO animals were included in the infarct size analysis using the intention to treat principle (**SI Appendix, Table S3**). For ultrasounds, data were excluded if one of the repeated measurements was missing resulting in 39 WT and 36 KO animals. The hemodynamic measurements were performed in 11WT and 16KO animals.

Long term study: For the permanent ischemia, from the 34 WT and 30 KO animals included in the study, 8 and 5 animals respectively died due to cardiac rupture or heart failure before the end of the experiment. The remaining 26 WT and 25 KO animals were included in the infarct size analysis using the intention to treat principle. For the transient model, 24 WT and 24 KO animals were included in the study of which 8 WT and 6 KO animals died before the end of the experiment. One WT and 1 KO animal could not be included in the infarct size analysis due to technical problems. The

remaining 15WT and 17KO mice were included according to intention to treat principle (**SI Appendix, Table S3**). For the ultrasounds, data were excluded if one of the repeated measurements was missing resulting in 21 WT and 23 KO animals for the permanent and 14WT and 16KO for the transient model. The hemodynamic measurements were performed in 20WT and 22KO animals for the permanent and 11WT and 15KO for the transient model, the other animals died just before or during the measurement due to heart failure.

Echocardiography

In vivo echocardiography measurements were performed under light isoflurane anaesthesia before the surgery and at day 1 (short term) or 14 and 28 (long term), using the Vevo 2100 echocardiography system (Visualsonics, Toronto, Canada). Two-dimensional B-Mode echocardiograms were captured at a rate of 90-120 Hz from parasternal long-axis views as well as from mid-papillary short axis-views of the left ventricle. Data were obtained from at least 3 different images taken in end-diastole and systole using the accompanying software from the Vevo 2100 echocardiography system. From the long-axis echocardiograms, the ejection fraction (EF) was defined as 100* (EDV-ESV)/EDV) (12, 13).

Evaluation of left ventricular contractility

Left ventricular contractility was measured at day 1 or 28 before sacrifice. Mice were anaesthetized with urethane 2.5mg/kg intraperitoneally (Sigma). Body temperature and respiration were controlled as described above. A high-fidelity pressure transducer (Mikro-tip, 1.4F, SPR-671 Millar Instruments, Houston, TX, USA) was inserted into the left ventricle via the right carotid artery. Ventricular pressure was measured and sampled at a rate of 2kHz. After a baseline measurement, the heart was stimulated by intravenous infusion of increasing doses of dobutamine (Sigma) via

a microinjection pump (Model 200 series, KdScientific, Boston, MA, USA) starting at 90µg/min and increasing by 90µg every two minutes to a maximum dose of 540µg/min. Heart rate, maximal positive pressure and minimal positive pressure were calculated for every infusion rate using IdeeQ software.

Evaluation of infarct size short term study

After reopening the chest, the left descending coronary artery was ligated again at the same spot. Then, Evans Blue ink was injected via the inferior vena cava and allowed to spread through the vascular system. Then, the hearts were quickly excised and frozen. After freezing, the hearts were cut into 4-5 slices of 2mm and soaked in TTC (2% in PBS) for 30 minutes. Pictures were taken with a Dinolite camera connected to the microscope. Area at risk and infarct size were were analysed using the Leica Qwin pro v3.5.1 software. Infarct sizes are expressed as percentage of total left ventricular area.

Evaluation of infarct size long term study

Infarct sizes were calculated from paraffin-embedded left ventricular sections stained with AZAN. Sections of 4µm were incubated in preheated AZAN I solution for 30 minutes at 37°C, followed by rinsing in demineralized water and incubation in 5% phosphotungstic acid for 45 minutes. After rinsing in tap water, slides were finally incubated in AZAN II solution (diluted 1:3 in demineralized water) for 10 minutes. Pictures were taken using a Leica camera connected to a Zeiss microscope. Pictures were analysed using the Leica Qwin pro v3.5.1 software. Infarct sizes are expressed as percentage area of the total left ventricular tissue area.

Hippocampal brain slices

In vitro damage caused by oxygen-glucose deprivation/re-oxygenation and the protection elicited by VAS2870 and GKT136901 was studied in acutely isolated rat

hippocampal slices. Brains from 2-3 months old adult male Sprague-Dawley rats (250-300 g) or Nox4 KO mice (2-3 months) were isolated as described previously (14). Rats or mice were quickly decapitated and forebrains were rapidly removed from the skull and placed into ice-cold Krebs bicarbonate dissection buffer (pH 7.4), containing (in mM): NaCl 120, KCl 2, $CaCl_2$ 0.5, $NaHCO_3$ 26, $MgSO_4$ 10, KH_2PO_4 1.18, glucose 11 and sucrose 200. The chamber solutions were pre-bubbled with either 95% O_2/5% CO_2 or 95% N_2/5% CO_2 gas mixtures, for at least 30 min before slice immersion, to ensure O_2 saturation or removal. The hippocampi were quickly dissected and 300mm thick slices were cut using a McIlwain Tissue Chopper. Then, the slices were transferred to vials containing a sucrose-free dissection buffer, bubbled with 95% O_2/5% CO_2 in a water bath at 37°C for 45 min, to allow tissue recovery (equilibration period). Oxygen and glucose deprivation was induced by incubating the slices for a 15 min period in a glucose-free Krebs solution (glucose was replaced by 2-deoxyglucose), equilibrated with a 95% N_2/5% CO_2 gas mixture. Slices incubated for 15 min in a modified Krebs solution (in mM: NaCl 120, KCl 2, $CaCl_2$ 2, $NaHCO_3$ 26, $MgSO_4$ 1.19, KH_2PO_4 1.18 and glucose 11), equilibrated with 95% O_2/5% CO_2 served as controls. After the OGD period, the slices were returned back to an oxygenated normal Krebs solution containing glucose for 2h (re-oxygenation period), during which VAS2870 (10 μM) or GKT136901 (0.1 μM) were added as treatments do the rat studies. In case of Nox4 KO mice, no treatment was used.

Cell viability of hippocampal slices

Hippocampal cell viability was determined using the colorimetric MTT assay (14). Hippocampal slices were collected immediately after the re-oxygenation period and were incubated with MTT (0.5 mg/ml) in Krebs bicarbonate solution for 30 min at 37°C. The tetrazolium ring of MTT can be cleaved by active dehydrogenases in viable cells,

producing a precipitated formazan derivative. This formazan derivative was solubilized by adding 200 μl DMSO. The optical density was measured spectrophotometrically at 540 nm using a micro plate reader. Absorbance values obtained in control slices were set to 100% viability and experimental variables were normalized with respect to this value.

ROS determination in hippocampal brain slices

To measure cellular reactive oxygen species (ROS), we used the molecular probe H_2DCFDA (34). Immediately after chopper sectioning, 300μm thick hippocampal slices were loaded with H_2DCFDA (10 $\mu l/ml$) for 40 min in Krebs solution. Subsequently, the slices were washed once with Krebs solution during 10 min and OGD/Re-Ox protocol started. Fluorescence was measured in each slice using a fluorescence inverted NIKON eclipse T2000-U microscope (Izasa, Madrid, Spain). Wavelengths of excitation and emission of H_2DCFDA were 485 and 520 respectively. Images were taken at CA1 at magnifications of 100x. Fluorescence analysis was performed using the Metamorph programme version 7.0. Fluorescence under basal conditions was set to 1 and experimental variables were normalized with respect to this value.

Human brain microvascular endothelial cells (HBMEC) culture subjected to hypoxia

HBME cells (Cell systems, USA) between passage 3 and 9 were cultured to approximately 90% confluence using specialized cell medium (EGM-2 MV BulletKit, Lonza, The Netherlands) enriched with 5% fetal bovine serum FBS before starting the hypoxia period. For cell studies, HBMECs were seeded at specific density ($6x10^4$ cells/ml) in 12 wells-plates and incubated during 24h at 37°C. Later, cell medium was replaced for non-FBS containing medium (2ml/well) following by 6h of hypoxia (94,8% N_2, 0.2% O_2 and 5% CO_2) at 37°C using hypoxia workstations (Ruskin Invivo2 400

station, The Netherlands). The hypoxia period was followed by 24h of reperfusion in presence or absence of 1 μM GKT136901 (Genkyotech, Switzerland) as treatment. Control cells were exposed to normoxia (75% N_2, 20% O_2 and 5% CO_2) and enriched medium during the hypoxia period. All flasks and well plates were pre-treated with fibronectin (Sigma-Aldrich, The Netherlands) solution (1:100 in PBS).

Assessment of cell viability in HBMEC

After 24h reperfusion, cell viability was assessed using the colorimetric MTT assay (14). MTT solution (5 mg/ml) was added to each well (100 μl/ml) and incubated for 2h at 37°C. The formazan salt formed was solubilized by adding 350 μl DMSO. The optical density was measured spectrophotometrically at 540 nm using a micro plate reader. Absorbance values obtained in control cells were set to 100% viability.

Cell permeability in HBMEC

For the passive diffusion assay 2 x 10^4 HBMEC were grown to confluence on membranes of Transwell inserts (collagen-coated Transwell Pore Polyester Membrane Insert; pore size = 3.0 μm (Greiner Bio One, Frickenhausen, Germany or Corning, The Netherlands). 24h before inducing 6h of ischemic conditions followed by 24h reperfusion period where cells were treated with 1μM GKT136901.

Dextran tracer: The passive permeability was assessed with 3kDa dextran tracer (fluorescein conjugated) and 70 kDa dextran tracer (Texas red conjugated) (Invitrogen, Waltham, MA USA). To load the tracer onto the HBMEC layer, the solution was removed from the upper and lower chamber of the Transwell system. The lower chamber was filled with ACSF solution (ACSF; 120 mM NaCl, 2.5 mM KCl, 1.25 mM NaH2PO4, 22 mM NaHCO3, 2 mM MgSO4, 2 mM CaCl2, and 20 mM glucose), the upper chambers with 25μg/ml tracer, diluted in ACSF solution. After 5 min incubation

at 37°C. The amount of diffused tracer in the lower chamber was measured with Tecan infinite M200PRO (TECAN, Männedorf, Switzerland).

Evans Blue extravasation: Cell permeability was assessed using the Evans Blue dye (Sigma-Aldrich, The Netherlands). To initiate the diffusion experiments, the medium was removed and cells were washed once with assay buffer. The same buffer (1.5 ml) was added to the abluminal side of the insert. Permeability buffer (0.5 ml) containing 4% bovine serum albumin (Sigma-Aldrich, The Netherlands) and 0.67 mg/ml Evans blue dye was loaded on the luminal side of the insert followed by 15 min incubation at 37°C. The concentration of Evans Blue in the abluminal chamber was measured by determining the absorbance of 150 µl buffer at 630 nm using a microplate reader.

Statistics

All mice and in vitro data are expressed as mean ± SEM. Rat in vivo experiments are expressed as mean ± SD. Using the GraphPad Prism 5.0 software package statistical differences between mean values were determined by Student's two-tailed t test (mice) and Mann-Whitney test for rat experiments. For repeated measurements a two-way ANOVA was used. Statistical comparisons between groups were performed using one-way ANOVA. Data were tested for Gaussian distribution with the D'Agostino and Pearson omnibus normality test and then analyzed by one-way analysis of variance (ANOVA) with posthoc Bonferroni adjustment for P values. The numbers of animals necessary to detect a standardized effect size on infarct volumes ≥ 0.2 were determined via a priori sample size calculation with the following assumptions: $\alpha = 0.05$, power of 80%, a minimal assessable treatment effect of 40% and a variation of 20% (GraphPad Stat Mate 2.0; GraphPad Software). Nonparametric functional outcome scores were compared by Kruskal-Wallis test with posthoc Dunn multiple

comparison test. For comparison of survival curves the log-rank test was used. P values < 0.05 were considered statistically significant.

Supplementary figures

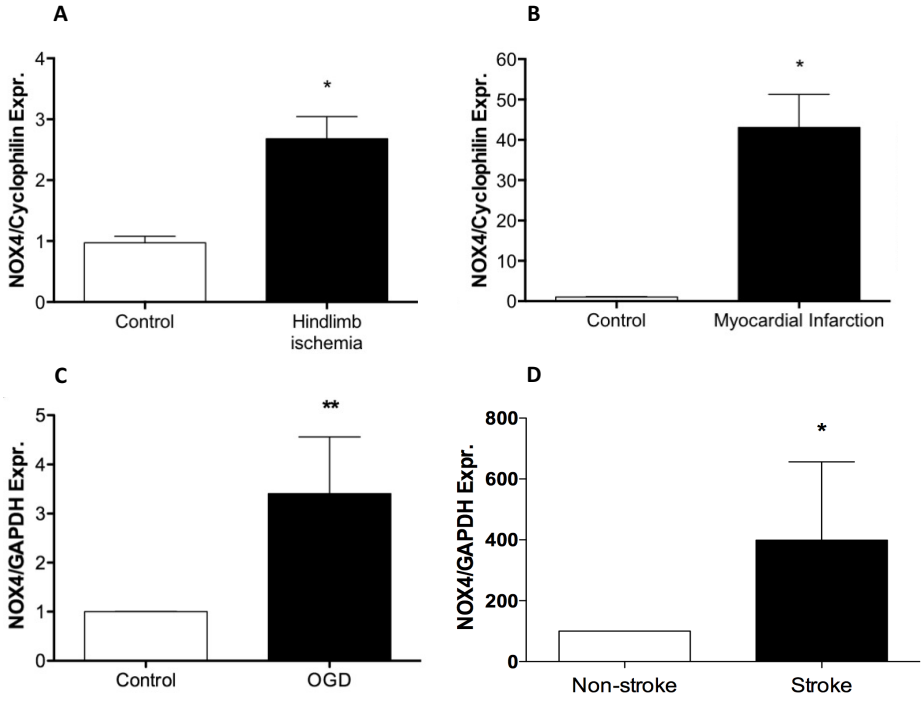

Figure S1. Induction of NOX4 expression in four different ischemic conditions: hindlimb ischemia, myocardial infarction, brain ischemia and a human brain microvascular endothelial cells (HBMEC) ischemia model. *(A)* Relative gene expression of *Nox4* was upregulated in wild type mice subjected to a permanent ligation of the femoral artery in comparison with sham-operated mice (* $P < 0.05$, control n = 6, hindlimb n = 10). *(B)* Relative gene expression of *Nox4* showed a 40 times increase in wild type mice subjected to occlusion of the left descending coronary artery compared to sham-operated mice (* $P < 0.05$, control n = 8, myocardial infarction n = 7). *(C) Nox4* gene expression in human brain microvascular endothelial cells (HBMEC) subjected to 6h of hypoxia (0.2% O_2) was significantly increased in comparison with HBMEC subjected to normoxia conditions (** $P < 0.01$, n = 5). *(D)* Nox4 expression in brain tissue from mice subjected to a transient occlusion of the middle cerebral artery (1h) was significantly increased in comparison with non-stroked animals (* $P < 0.05$, stroke n = 4, non-stroke n = 4).

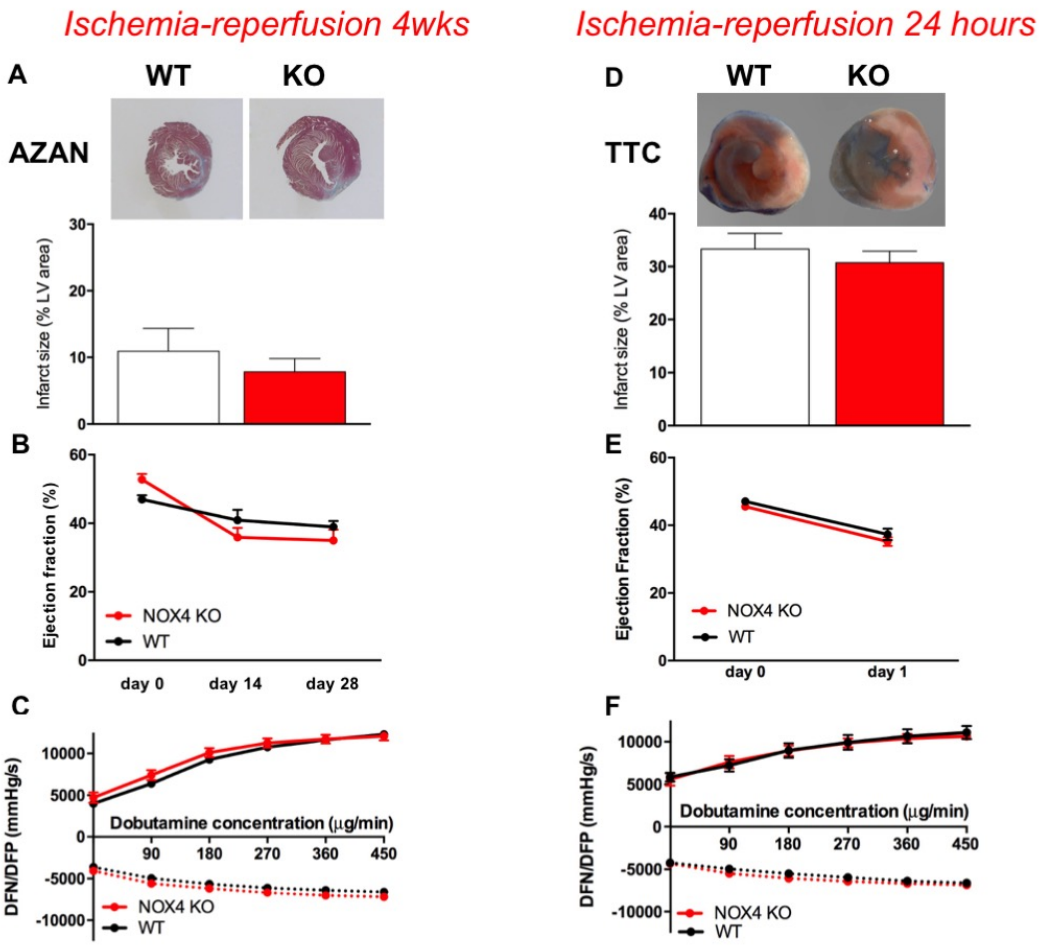

Figure S2. Role of NOX4 in ischemia-reperfusion of the heart on long term (A/B/C) and short term (D/E/F) effects. *(A)* No significant differences in infarct size 4 weeks after ischemia-reperfusion between Nox4 KO (red, n = 17) and WT mice (black, n = 15). *(B)* Ejection fraction decreased after heart ischemia-reperfusion showed no significant change between Nox4 KO (red, n = 16) and WT mice (black, n = 14). *(C)* Left ventricular function was not different between NOX4 KO (red, n=15) and WT mice (black, n =11). *(D)* No significant differences in infarct size 24h after ischemia-reperfusion between Nox4 KO (red, n = 16) and WT mice (black, n = 17). *(E)* Ejection fraction decreased after heart ischemia-reperfusion with no significant change between Nox4 KO (red, n = 36) and WT mice (black, n = 39). *(F)* Left ventricular

function was not different between Nox4 KO (red, n = 16) and WT mice (black, n = 11). Representative staining pictures are shown above each graph.

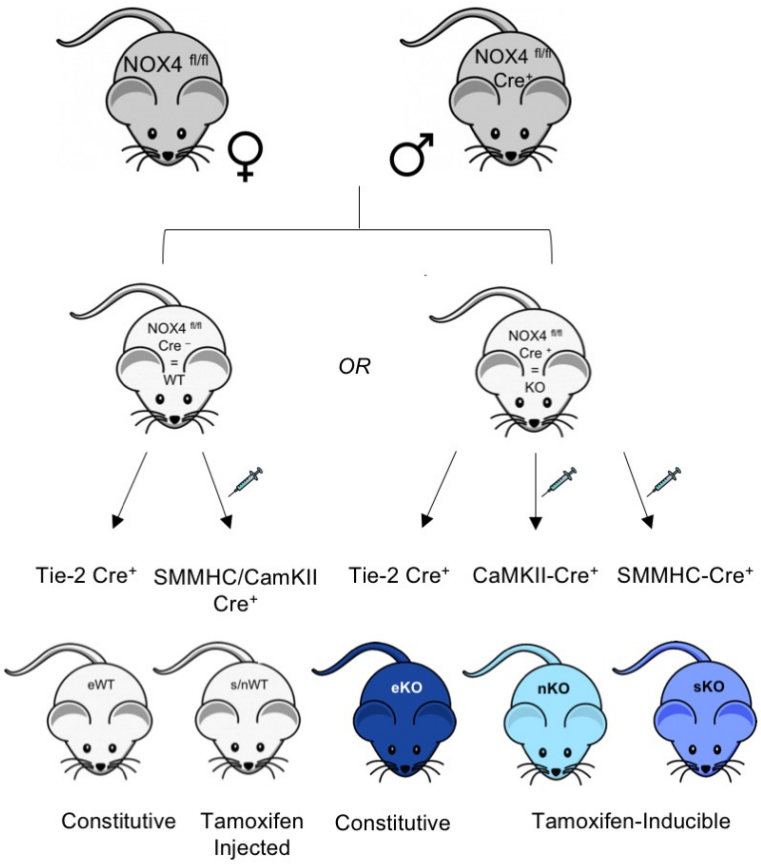

Figure S3. Generation of cell-specific Nox4 KO mice. For endothelial-cell specific NOX4 KO mice (eKO, dark blue), female mice homozygous for the floxed NOX4 gene were bred with normal C57/Bl6 male mice that express the Cre recombinase gene under control of the endothelial-cell specific Tie2 promotor. Smooth muscle cell-specific (sKO, intermediate blue) and neuron specific Nox4 KO (nKO, light blue) mice were generated in an analogous way using SMMHC-Cre+ mice and CaMKII-Cre+ mice respectively. Deletion of Nox4 in SMC and neurons was Tamoxifen-inducible. sWT and nWT mice were also injected with Tamoxifen for proper comparison.

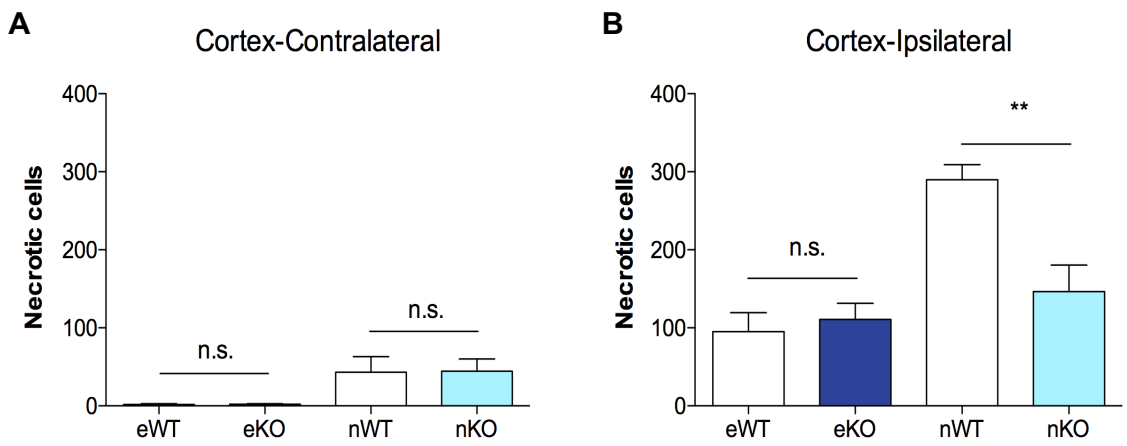

Figure S4. Contribution of endothelial and neuronal NOX4 in necrosis. *(A)* Contralateral side: No difference in number of cortical necrotic neurons was found in endothelial Nox4 KO (eKO) and neuronal Nox4KO (nKO) mice in comparison with WT animals. *(B)* Ipsilateral side: nKO mice presented less necrotic cells in comparison with nWT (** $P < 0.01$, $n = 8$) while no effect was shown in eKO mice ($n = 8$).

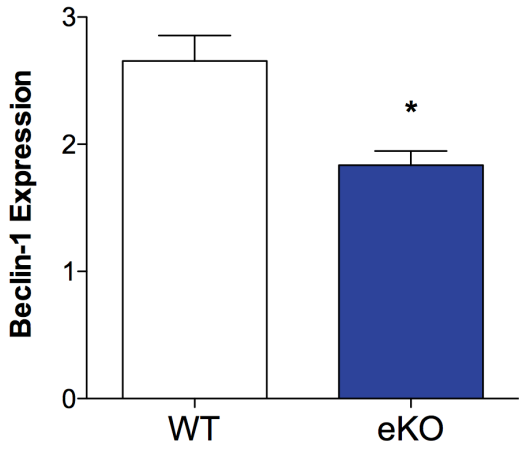

Figure S5. Protein expression of beclin-1 in brain tissue from endothelial NOX4 KO (eKO) and WT mice post-stroke. Significant reduction of beclin-1 protein expression after brain ischemia (tMCAO) has been found in eKO mice compared to their respective WTs mice (* $P < 0.05$, $n = 6$).

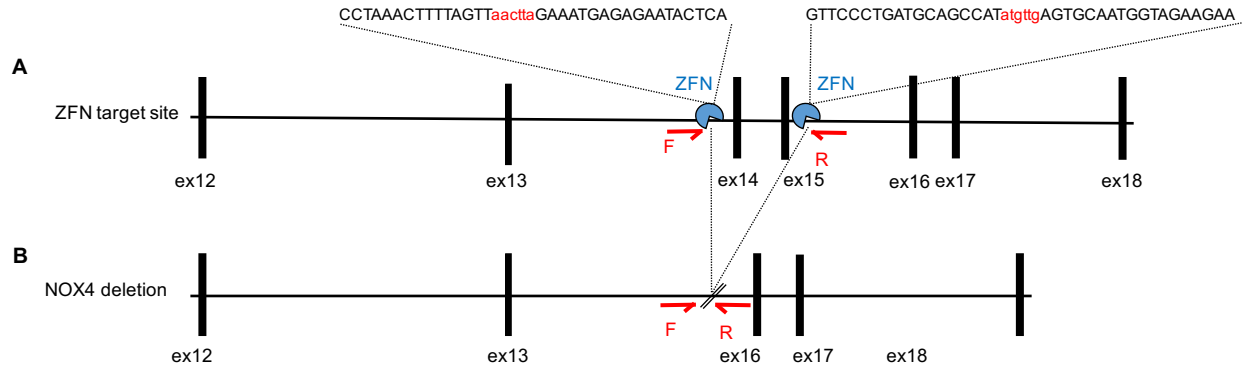

Figure S6. Nox4 KO rat generation. *(A)* Microinjections of Zinc Finger Nucleases (ZFN) pairs targeting exon 14 and 15 into wildtype female WKY rats resulted in the respective loss of exons 14 and 15. Specific NOX4 ZFN-binding sequence (red) and ZFN cleavage site (blue). *(B)* Representation of the Nox4 KO deletion product. Flanking primers for the deletion regions, forward and reverse are represented in red (F and R).

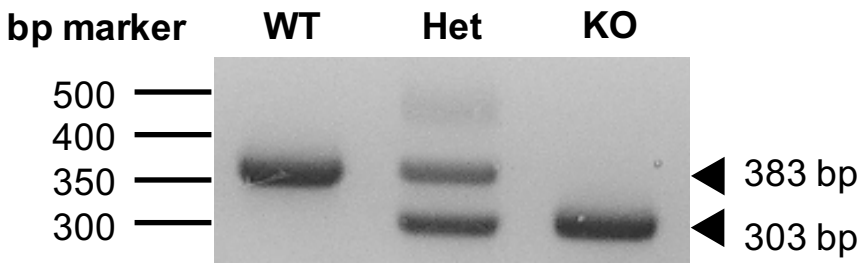

Figure S7. NOX4 KO rat genotyping. Control and Nox4 KO rat tail genomic DNA were purified and a PCR was performed to amplify the sequence covering exons 14 and 15 of the Nox4 gene (See material and methods for details). WT animals showed the complete DNA fragment (383bp) while in KO rats the mutated gene was detected (303bp). Both WT and KO bands were shown in heterozygote animals.

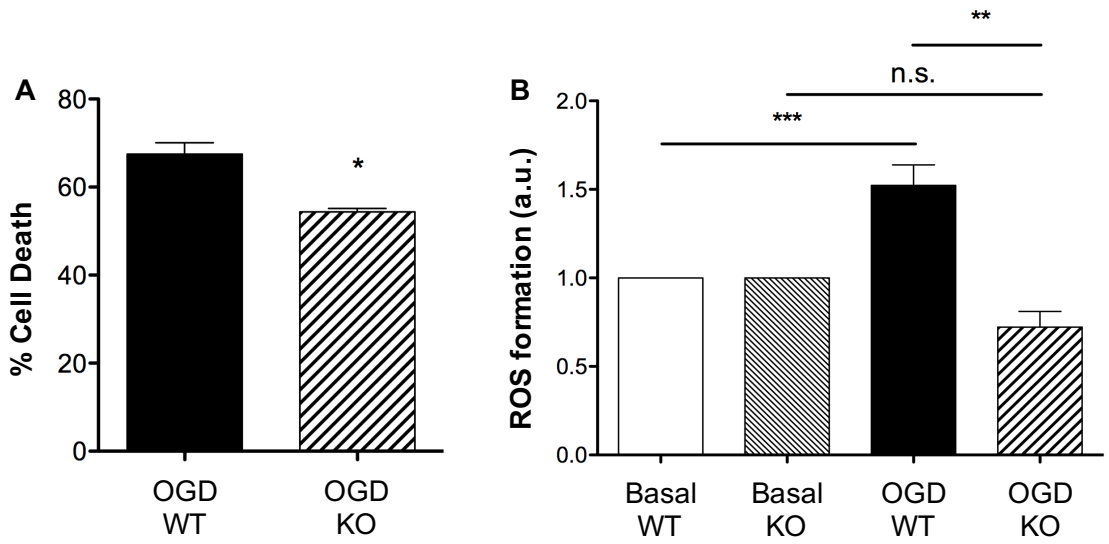

Figure S8. **Cell death and ROS formation are significantly reduced in hippocampal brain slices from Nox4 KO mice.** *(A)* Cell death was significantly reduced in hippocampal brain slices from global Nox4 KO mice compared to its respective WT littermates (* $P < 0.05$, $n = 4$). *(B)* ROS formation was also decreased in hippocampal brain slices subjected to OGD in comparison with WT OGD-treated slices (** $P < 0.01$, *** $P < 0.001$, $n = 4$).

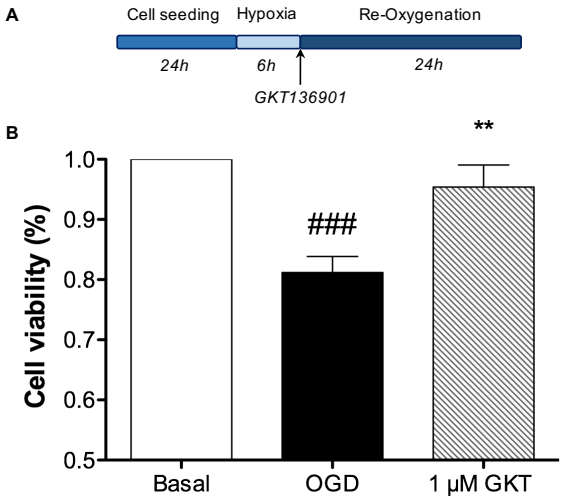

Figure S9. GKT136901 increases cell viability in human brain microvascular endothelial cells (HBMEC) subjected to OGD/Re-oxygenation (Re-Ox). *(A)* Experimental protocol. To promote cell seeding, HBMEC were incubated during 24h under physiological conditions followed by 6h of hypoxia period and 24h of Re-Ox. 1 μM GKT136901 was added at the beginning of the the Re-Ox period (time=0 after hypoxia). *(B)* Cell viability was significantly increased in cells treated with 1 μM GKT136901 (** $P < 0.01$, $n = 6$) in comparison with non-treated cells ($^{###} P < 0.001$, $n = 6$).

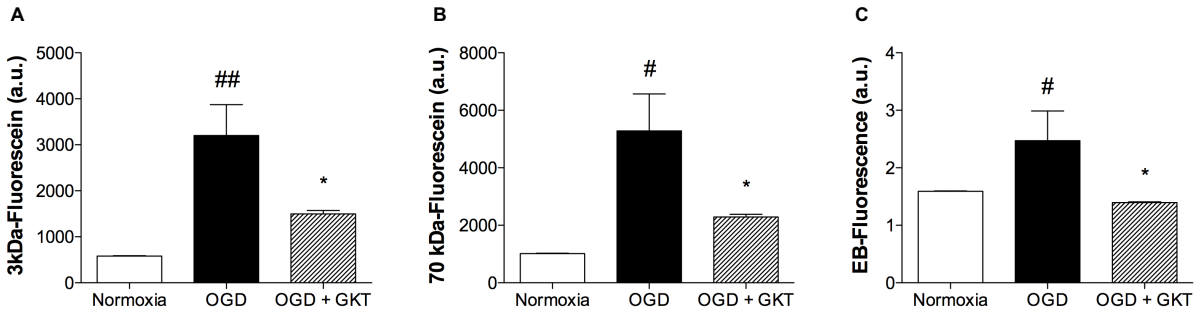

Figure 10. Effects of GKT136901 treatment on dextran tracer and Evans Blue (EB) permeability in human brain microvascular endothelial cells (HBMEC) subjected to hypoxia/Re-oxygenation (Re-Ox). *(A)* Passive permeability was assessed with a 3 kDa dextran tracer (fluorescein conjugated) and *(B)* a 70 kDa dextran tracer after 6h of hypoxia followed by 24h of re-oxygenation period in presence or absence of 1 µM GKT136901. Cell permeability was significantly increased after OGD ($^{\#\#}$ $P < 0.01$, $^{\#}$ $P < 0.05$, $n = 5$) while NOX4 inhibition post-OGD prevented this detrimental effect (* $P < 0.05$, $n = 5$). *(C)* Cell permeability was also assessed by measuring EB fluorescence post-OGD. EB diffusion was significantly reduced in treated cells (1 µM GKT136901) ($^{\#}$ $P < 0.05$, $n = 3$) in comparison with non-treated cells (* $P < 0.05$, $n = 3$).

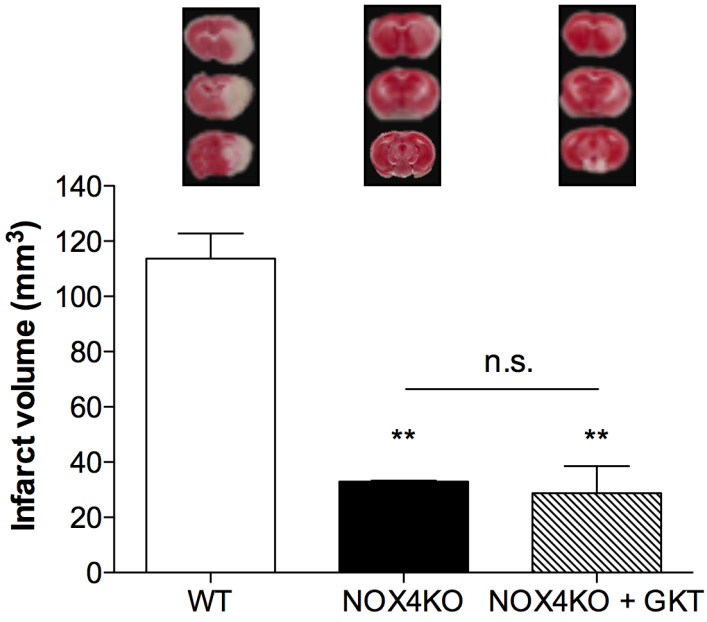

Fig S11. GKT136901 treatment after 1h occlusion of the middle cerebral artery (tMCAO) in Nox4 KO mice. Infarct volume was significantly reduced in Nox4 KO (no treatment) and Nox4 KO animals treated with GKT136901 (10 mg/Kg) in comparison with WT mice (** $P < 0.01$, $n = 5$). No difference was detected when comparing Nox4 KO ($n = 3$) and Nox4 KO mice ($n = 3$) treated with GKT136901 (10 mg/Kg) after 1h tMCAO. Complete sets of brain slices from a representative animal (TTC staining) are shown above the graph.

Supplementary tables

Table S1. NOX4 gene expression in bone marrow of WT and Tie2-Cre mice

	WT mice NOX4 expression	**WT mice NOX2 expression**	**WT mice ß-actin**
Animal number	*Ct*	*Ct*	*Ct*
1	-	23,49	17,79
2	-	32,05	26,55
3	-	25,21	18,95
4	-	22,54	17,47
5	-	22,23	17,87
6	-	23,44	18,01
	Tie2-Cre mice NOX4 expression	**Tie2-Cre mice NOX2 expression**	**Tie2-Cre mice ß-actin**
Animal number	*Ct*	*Ct*	*Ct*
1	38,42	23,55	17,54
2	-	24,59	19,15
3	-	25,42	18,79
4	-	23,12	16,72
5	-	21,26	16,34
6	-	23,25	17,48

NOX, NADPH oxidase, WT, wild type.

Table S2. mRNA levels of NOX1, NOX2 and NOX4 in brain, kidney and lung samples from NOX4 KO/WT rats

		NOX4			
WT Sample	*Ct*	*KO Sample*	*Ct*	*ΔCt*	$-2^{\Delta Ct}$
WT - Brain	34.75	KO - Brain	-	-	-
WT - Lung	27.57	KO - Lung	-	-	-
WT - Kidney	29.15	KO - Kidney	-	-	-
		NOX1			
WT Sample	*Ct*	*KO Sample*	*Ct*	*ΔCt*	$-2^{\Delta Ct}$
WT - Brain	37.10	KO - Brain	33.87	3.23	0.106668096
WT - Lung	37.45	KO - Lung	37.29	0.16	0.897605695
WT - Kidney	-	KO - Kidney	-	-	-
		NOX2			
WT Sample	*Ct*	*KO Sample*	*Ct*	*ΔCt*	$-2^{\Delta Ct}$
WT - Brain	34.23	KO - Brain	32.42	1.81	0.285396759
WT - Lung	26.56	KO - Lung	27.46	-0.89	1.85891441
WT - Kidney	31.73	KO - Kidney	32.09	-0.36	1.281437078
		Internal control – ß-actin			
WT Sample	*Ct*	*KO Sample*	*Ct*	*ΔCt*	$-2^{\Delta Ct}$
WT - Brain	19.84	KO - Brain	19.05	0.78	0.580647042
WT - Lung	20.81	KO - Lung	19.28	1.53	0.34706622
WT - Kidney	21.51	KO - Kidney	21.41	-0.82	1.763199399

NOX, NADPH oxidase, WT, wild type; KO, Knock-out.

Table S3. Animals excluded from the statistical analysis after tMCAO, myocardial infarction and hindlimb ischemia

Animals	Ischemia model	Experiment Duration	Excluded Animals
C57/Bl6N	tMCAO	24h	2 of 15
NOX4 KO	tMCAO	24h	4 of 16
C57/Bl6N	Ischemia-reperfusion	24h	2 of 19 (infarct size)
NOX4 KO	Ischemia-reperfusion	24h	2 of 18 (infarct size)
C57/Bl6N	Ischemia-reperfusion	28 days	9 of 24
NOX4 KO	Ischemia-reperfusion	28 days	7 of 24
C57/Bl6N	Myocardial infarction	28 days	8 of 34
NOX4 KO	Myocardial infarction	28 days	5 of 29
C57/Bl6N	Hindlimb ischemia	28 days	2 of 25
NOX4 KO	Hindlimb ischemia	28 days	0 of 17
eWT	tMCAO (TTC)	24h	6 of 31
eNOX4 KO	tMCAO (TTC)	24h	5 of 32
s/nWT	tMCAO (TTC)	24h	1 of 38
sNOX4 KO	tMCAO (TTC)	24h	1 of 10
nNOX4 KO	tMCAO (TTC)	24h	3 of 23
eWT	tMCAO (Evans blue)	24h	2 of 10
eNOX4 KO	tMCAO (Evans blue)	24h	4 of 10
nWT	tMCAO (Evans blue)	24h	3 of 10
nNOX4 KO	tMCAO (Evans blue)	24h	3 of 10
WKY rats	tMCAO (TTC)	24h	1 of 12
NOX4 KO rat	tMCAO (TTC)	24h	2 of 11

NOX4, NADPH oxidase 4; WT, wild type; KO, Knock-out; sNOX4, smooth muscle cells NOX4 KO; nNOX4, neuronal NOX4 KO; eNOX4 KO, endothelial NOX4 KO; tMCAO, transient occlusion of the middle cerebral artery; TTC, 2,3,5- triphenyltetrazolium hydrochloride.

Animal exclusion procedures are described in the respective methods parts.

References

1. Kleinschnitz C, et al. (2010) Post-stroke inhibition of induced NADPH oxidase type 4 prevents oxidative stress and neurodegeneration. *PLoS Biol* 8(9):e1000479.

2. Wirth A, et al. (2008) G12-G13-LARG-mediated signaling in vascular smooth muscle is required for salt-induced hypertension. *Nat Med* 14(1):64–68.

3. Casanova E, et al. (2001) A CamKIIalpha iCre BAC allows brain-specific gene inactivation. *Genesis* 31(1):37–42.

4. Groneberg D, et al. (2010) Smooth Muscle-Specific Deletion of Nitric Oxide-Sensitive Guanylyl Cyclase Is Sufficient to Induce Hypertension in Mice. *Circulation* 121(3):401–409.

5. Göb E, et al. (2015) Blocking of plasma kallikrein ameliorates stroke by reducing thromboinflammation. *Annals of Neurology* 77(5):784–803.

6. Bederson JB, et al. (1986) Evaluation of 2,3,5-triphenyltetrazolium chloride as a stain for detection and quantification of experimental cerebral infarction in rats. *Stroke* 17(6):1304–1308.

7. Kraft P, Schwarz T, Pochet L, Stoll G, Kleinschnitz C (2010) COU254, a specific 3-carboxamide-coumarin inhibitor of coagulation factor XII, does not protect mice from acute ischemic stroke. *Exp Transl Stroke Med* 2(1):5.

8. Bederson JB, et al. (1986) Rat middle cerebral artery occlusion: evaluation of the model and development of a neurologic examination. *Stroke* 17(3):472–476.

9. Moran PM, Higgins LS, Cordell B, Moser PC (1995) Age-related learning deficits in transgenic mice expressing the 751-amino acid isoform of human beta-amyloid precursor protein. *Proceedings of the National Academy of Sciences* 92(12):5341–5345.

10. Langhauser F, et al. (2012) Kininogen deficiency protects from ischemic neurodegeneration in mice by reducing thrombosis, blood-brain barrier damage, and inflammation. *Blood* 120(19):4082–4092.

11. Vine DL, Dodge HT, Frimer M, Stewart DK, Caldwell J (1976) Quantitative measurement of left ventricular volumes in man from radiopaque epicardial markers. *Circulation* 54(3):391–398.

12. Egea J, et al. (2007) Neuroprotection afforded by nicotine against oxygen and glucose deprivation in hippocampal slices is lost in alpha7 nicotinic receptor knockout mice. *Neuroscience* 145(3):866–872.

13. Maroto M, et al. (2011) Multi-target novel neuroprotective compound ITH33/IQM9.21 inhibits calcium entry, calcium signals and exocytosis. *Cell Calcium* 50(4):359–369.

14. Denizot F, Lang R (1986) Rapid colorimetric assay for cell growth and survival. Modifications to the tetrazolium dye procedure giving improved sensitivity and reliability. *J Immunol Methods* 89(2):271–277.